Fermi and Swift Gamma-ray Burst Afterglow Population Studies

Judith L. Racusin (NASA/GSFC), Samantha Oates (MSSL-UCL)

Abstract

The new and extreme population of GRBs detected by Fermi-LAT shows several new features in high energy gamma-rays that are providing interesting and unexpected clues into GRB prompt and afterglow emission mechanisms. Over the last 6 years, it has been Swift that has provided the robust data set of UV/optical and X-ray afterglow observations that opened many windows into components of GRB emission structure. The relationship between the LAT GRBs and the well studied, fainter, less energetic GRBs detected by Swift-BAT is only beginning to be explored by multi-wavelength studies. We explore the large sample of GRBs detected by BAT only, BAT and Fermi-GBM, and GBM and LAT, focusing on these samples separately in order to search for statistically significant differences between the populations, using only those GRBs with measured redshifts in order to physically characterize these objects. We disentangle which differences are instrumental selection effects versus intrinsic properties, in order to better understand the nature of the special characteristics of the LAT bursts.

Motivation

Using the large X-ray and optical afterglow data sets from the Swift GRB observations (XRT - Racusin et al. 2009, UVOT - Oates et al. 2009) from 2004-2009, we survey the populations of the BAT, GBM, and LAT detected GRBs with measured redshifts. Using both prompt emission and afterglow observations of these samples, we study the differences between their intrinsic properties and instrumental selection effects.

GRB Samples

The BAT sample are those GRBs originally discovered by Swift-BAT and not detected by Fermi-GBM or LAT. Many of these bursts occurred prior to the Fermi launch (June 2008).

The GBM sample are those GRBs detected by both GBM and BAT. Follow-up observations are not possible for GBM-only bursts due to the large position errors from GBM (~few deg). Therefore, all GBM bursts in this study were also observed by BAT.

The LAT sample are those GRBs detected by LAT and GBM, and in the case of GRB 090510, all three instruments. Ten of the 20 detected LAT GRBs have had sufficient statistics to provide ~arcmin error circles for Swift follow-up at times > 12 hours. Of those 10, 8 were detected by XRT, and 7 by UVOT, including the one simultaneous trigger (GRB 090510). All 8 led to redshift determinations by ground-based telescopes. Observations of LAT emission were not simultaneous with the lower energy afterglow observations (except for GRB 090510).
The number of GRBs in each sample after making cuts on data usability are listed in Table 1.

Table 1: The number of GRBs in each of the BAT, GBM, and LAT samples with well populated light curves in the XRT and UVOT data. All of the GRBs in out samples have measured redshifts.

Sample Statistics		
	XRT	UVOT
BAT	147	49
GBM	19	11
LAT	8	5

Luminosity

Using the X-ray (0.3-10 keV) and u-band normalized light curves, and redshift information, we create rest frame light curves for the BAT, GBM, and LAT samples (Figure 1 & 2). We compare these luminosities at times of 11 hours and 1 day, and find that in both the X-ray and optical, the LAT and GBM bursts are more clustered than the BAT bursts but well within the normal BAT sample distributions, and are slightly above the median luminosity.

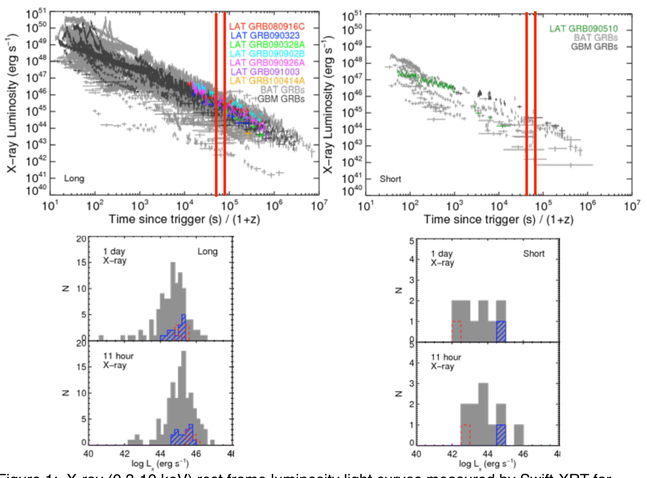

Figure 1: X-ray (0.3-10 keV) rest frame luminosity light curves measured by Swift-XRT for the BAT, GBM, and LAT samples. The top panels show the long (left) and short (right) burst light curves. The lower plots show histograms of the luminosities at 11 hours and 1 day (rest frame) for the long (lower left) and short (lower right) bursts.

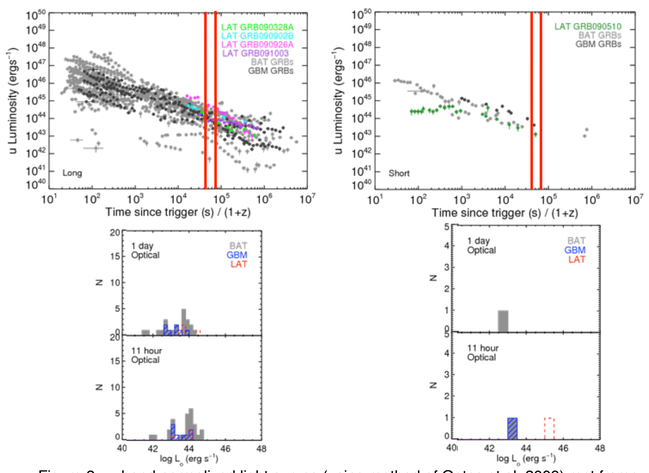

Figure 2: u-band normalized light curves (using method of Oates et al. 2009) rest frame luminosity light curves measured by Swift-UVOT for the BAT, GBM, and LAT samples. The top panels show the long (left) and short (right) burst light curves. The lower plots show histograms of the luminosities at 11 hours and 1 day (rest frame) for the long (lower left) and short (lower right) bursts.

Redshift

All 174 GRBs in this study have had either measured spectroscopic or accurate photometric redshifts (Figure 3). The *Swift* GRBs have a different redshift distribution than pre-*Swift* samples (Jakobsson et al. 2006), therefore it should follow that other GRB populations discovered with different gamma-ray instruments, could have different redshift distributions. Yet we find that there are no statistical differences between our samples (when splitting long and short bursts). The GBM sample is a subset of the BAT sample, and there are only 8 LAT GRBs, therefore, this may not be entirely unexpected.

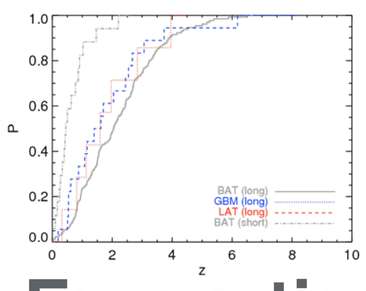

Figure 3: Cumulative redshift distribution for the BAT, GBM, and LAT long GRB samples, as well as the short BAT GRB sample. A K-S test shows that there are no significant differences between the long burst distributions, and there are insufficient statistics to compare the short GBM and LAT distributions.

Energetics

We use the prompt emission spectral information and the redshift measurements to calculate the isotropic equivalent gamma-ray energy output ($E_{\gamma,iso}$). We use the method described in Racusin et al. (2009) to estimate $E_{\gamma,iso}$ for bursts with only BAT observations of their prompt emission.

The LAT long duration GRBs have systematically high $E_{\gamma,iso}$ values than the BAT or GBM samples (Figure 4). The LAT bursts are among the most energetic GRBs ever observed. The high values of E_{peak} in the LAT bursts, which in turn leads to a more likely detection in the LAT band, and high $E_{\gamma,iso}$ values qualitatively follow the expectations of the empirical E_{peak}-$E_{\gamma,iso}$ relation (Amati et al. 2002).

Figure 4: $E_{\gamma,iso}$ distributions for the BAT, GBM, and LAT samples split into long and short GRBs. The LAT long bursts are on average more energetic than the other samples.

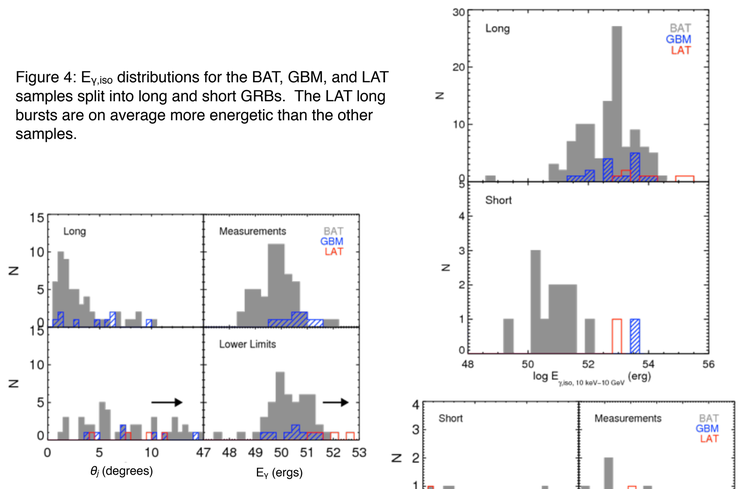

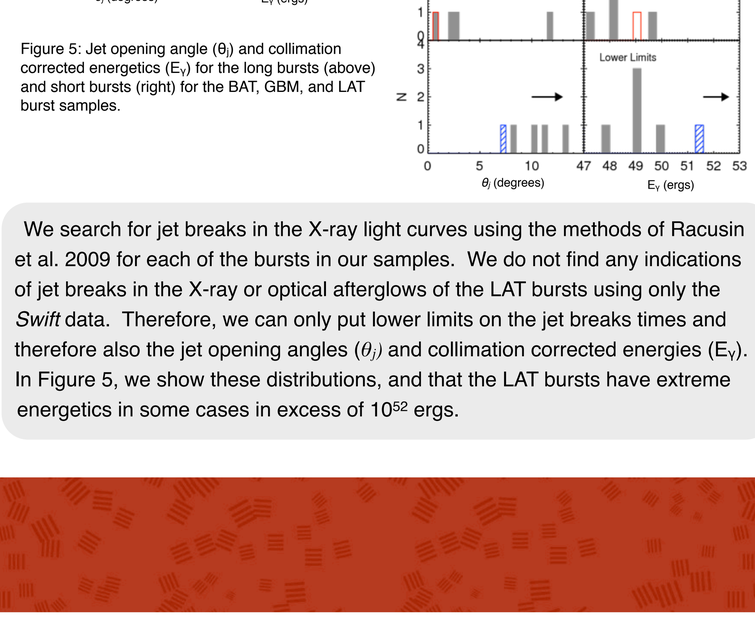

Figure 5: Jet opening angle (θ_j) and collimation corrected energetics (E_γ) for the long bursts (above) and short bursts (right) for the BAT, GBM, and LAT burst samples.

We search for jet breaks in the X-ray light curves using the methods of Racusin et al. 2009 for each of the bursts in our samples. We do not find any indications of jet breaks in the X-ray or optical afterglows of the LAT bursts using only the *Swift* data. Therefore, we can only put lower limits on the jet breaks times and therefore also the jet opening angles (θ_j) and collimation corrected energies (E_γ). In Figure 5, we show these distributions, and that the LAT bursts have extreme energetics in some cases in excess of 10^{52} ergs.

Radiative Efficiency

To learn about the physical differences between the samples, we used the observed quantities to calculate parameters such as the kinetic energy and radiative efficiency. The kinetic energy can be inferred from the X-ray afterglow during the normal forward shock phase using the method described by Zhang et al. 2007. In Figure 6, we show the kinetic energy (E_k) versus the isotropic equivalent gamma-ray energy ($E_{\gamma,iso}$) and derive the radiative efficiency (the efficiency at turning the kinetic energy of the shock wave into gamma-ray photons).

$$\eta = \frac{E_{\gamma,iso}}{E_{\gamma,iso} + E_k}$$

The BAT and GBM burst samples behave similarly to the small sample of *Swift* detected GRBs and XRFs analyzed in Zhang et al. 2007. However, the LAT bursts have on average higher radiative efficiencies, which fits into the picture that they have extreme energetics, but normal afterglows. The (in some cases) > 90% efficiency seems unrealistic, and may be an indication of a more complicated physical process than the simple synchrotron fireball model, or extreme conditions like Poynting flux dominated jets.

Figure 6: Kinetic Energy (E_k) versus the isotropic equivalent gamma-ray energy ($E_{\gamma,iso}$) for the BAT, GBM, and LAT bursts for which we have enough information to calculate these parameters. The diagonal lines indicate different values of the radiative efficiency (η). On average, the LAT burst sample have larger radiative efficiencies.

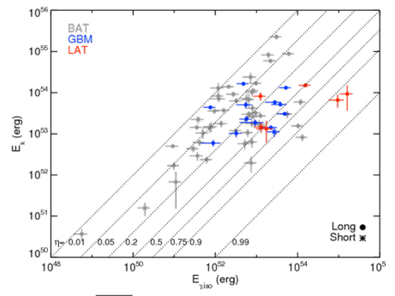

Bulk Lorentz Factors

Another fundamental difference between the LAT GRB sample and typical Swift era bursts are the high bulk Lorentz factors (Γ). However, there are several different and often contradictory methods for determining Γ. In Figure 7, we plot 4 different methods and their detections, upper, or lower limits for individual bursts in each sample. The methods are the γγ pair production attenuation limits (Lithwick & Sari 2001, Abdo et al. 2009), the forward shock peak estimation from the optical light curves (Sari & Piran 1999, Molinari et al. 2007),the limit on forward shock contribution to the sub-MeV prompt emission (Zou & Piran 2010), and the 2-zone γγ pair production attenuation method assuming the sub-MeV and GeV photon come from physical regions (Zou et al. 2010).

Although the different methods cannot be applied to every bursts, if we believe that all methods are valid, the general trend is that the LAT bursts have Γ of order a factor of ~2 larger than the BAT or GBM bursts.

Figure 7: Limits on the bulk Lorentz factor (Γ) for individual bursts in the BAT, GBM, and LAT samples using the 4 methods described above. In most cases, the methods yield consistent results, but the overall trend is that the LAT bursts have higher Γ.

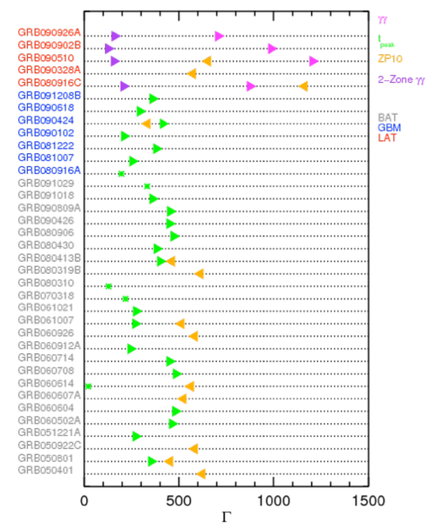

Conclusions

We survey the observational properties and derive theoretical implications of the BAT, GBM, and LAT populations in order to distinguish physical differences between them, and to put the extreme LAT bursts in the context of the well studied Swift sample collected over the last 6 years.

In addition to the new high energy components observed in the LAT GRBs, they have some of the most energetic prompt emissions ever observed, yet they have very typical afterglow properties. Using a combination of the observed prompt emission properties and the jet opening angle limits from the afterglows, we put lower limits on the total gamma-ray energy of the LAT bursts and their energetics lower limits remain at the extreme of the distribution. The LAT GRB sample also appears to have higher radiative efficiencies and bulk Lorentz factors that their less energetic counterparts in the BAT and GBM samples.

The exciting population of LAT detected GRBs have several different underlying properties that other GRB populations, which appear to not entirely be instrumental selection effects. How the production of high energy (GeV) gamma-rays in a GRB are somehow related to the high radiative efficiency and bulk Lorentz factors remains unclear. More broadband observations of these objects will help to shed light onto this subject.

More details will be presented in Racusin et al. (2011, submitted to ApJ).